

# Improving abdomen tumor low-dose CT images using dictionary learning based patch processing and unsharp filtering

Chen Yang<sup>1 2 3 \*</sup> [chenyang.list@seu.edu.cn](mailto:chenyang.list@seu.edu.cn), Fei Yu<sup>3</sup>, Limin Luo<sup>2 3</sup>, Christine Toumoulin<sup>1 2 \*</sup>

<sup>1</sup> LTSI, Laboratoire Traitement du Signal et de l'Image INSERM : U1099, Université de Rennes 1, Campus Universitaire de Beaulieu - Bât 22 - 35042 Rennes, FR

<sup>2</sup> CRIBS, Centre de Recherche en Information Biomédicale sino-français INSERM : Laboratoire International Associé, Université de Rennes 1, SouthEast University, 9 Rue Jean Macé, 35700 Rennes, FR

<sup>3</sup> LIST, Laboratory of Image Science and Technology [Nanjing] SouthEast University, School of Computer Science and Engineering, Si Pai Lou 2, Nanjing, 210096, CN

\* Correspondence should be addressed to: Chen Yang <[chenyang20071979@hotmail.com](mailto:chenyang20071979@hotmail.com)>

\* Correspondence should be addressed to: Christine Toumoulin <[christine.toumoulin@univ-rennes1.fr](mailto:christine.toumoulin@univ-rennes1.fr)>

## Abstract

Reducing patient radiation dose, while maintaining a high-quality image, is a major challenge in Computed Tomography. The purpose of this work is to improve abdomen tumor low-dose CT (LDCT) image quality by using a two-step strategy: a first patch-wise non linear processing is first applied to remove the noise, that is based on a sparsity prior in term of a learned dictionary, then an unsharp filtering aims to enhance the contrast of tissues and compensate the contrast loss caused by the DL processing. Preliminary results show that the proposed method is effective in suppressing mottled noise as well as improving tumor detectability.

**Author Keywords** X-ray CT, Image denoising, Image enhancement

## INTRODUCTION

CT imaging is increasingly incorporated into clinical decision making and despite rapid progresses in CT technology over the past decade, one major concern appears today related to the associated radiation rate rising [1–2]. A large number of researches in CT have been motivating by the need to reduce patient radiation dose. Among the possible solutions, one is to consider lowering the X-ray tube current. Nevertheless, low dose CT provides degraded images by mottled noise and different kinds of non stationary artifacts [3–4], which render the interpretation of these images particularly difficult. Tumor tissues often thus appear under the form of mosaic shapes within a low contrasted environment [5–6]. Two kinds of methods are applied to enhance image quality. They, either, directly proceed in the reconstruction domain or within a postprocessing denoising stage. In both cases, efficient noise suppression and tumor tissue preservation remains challenging. Neighborhood filters have shown interesting properties for the restoration of noisy low dose CT images. Let cite for instance, adaptive filters [6] that allow to reduce the X-ray dose by 50% for the same image quality and without loss in low contrast detectability. Other filters such as multiscale penalized weighted least-squares [7], bilateral filters [8] and Non Local Mean (NLNM) [9] have also shown some efficiency in enhancing anatomical/ pathological features in Low dose CT images.

Recent years have reported a growing interest in the study of sparse representation based dictionary learning (DL) [10–14]. Compared to pixel-wise intensity update-based restoration methods, patch-wise DL processing are considered as being more robust to mottled noise and generally provides a more efficient representation of patch-shaped features such as tumors or organs.

We describe in this paper, a new patch-wise processing, based on a sparsity prior in terms of a learned dictionary to suppress mottled noises in abdomen tumor LDCT images and a contrast-enhancing unsharp filter whose role is to compensate the contrast loss induced by the DL process. This method referred as **DL-unsharp** algorithm, is described in section 2. The flowchart of the method is given in Fig. 1. Section 3 provides a comparative study between our algorithm and a NLNM restoration filter [9]. Preliminary results show that the proposed DL-unsharp algorithm provides a good restoration of structures in LDCT images with an image quality that is comparable with the original SDCT images.

## METHOD

The core idea is to impose a sparsity prior patch-wise on the LDCT images in terms of a *dictionary*  $\mathbf{D}$ . Assuming the patches in the LDCT image are sparsely representable, DL based patch processing is carried out by coding each patch as a linear combination of just a few patches in the dictionary i.e. each patch of the image can be approximated by a linear combination of just a few columns from  $\mathbf{D}$  [1–12]. This way to proceed leads to find the best global over-complete dictionary. The coefficients of the linear combination can be estimated through the sparse coding process described in [13].

The DL based patch processing aims to solve the following optimization problem [14]:

$$\min_{x, D, \Gamma} \|x - y\|_2^2 + \mu \sum_{ij} \|R_{ij}x - D\alpha_{ij}\|_{2, \sigma}^2 \quad \text{s.t. } \|\alpha_{ij}\|_0^0 \leq L_0 \forall i, j$$

(1)

where,  $x$  and  $y$  denote the treated and original LDCT images, respectively.  $R$  is the operator that extracts the square patch  $x$  of size  $\sqrt{n} \times \sqrt{n}$  (centered at point  $(i, j)$ ) from the image  $x$ . This patch is encoded by  $D\alpha$  as a  $n \times K$  matrix, which is composed by  $K$  columns of  $n$ -vectors. Each  $n$ -vector column corresponds to a patch of size  $\sqrt{n} \times \sqrt{n}$ .  $\Gamma$  denotes the coefficient set  $\{\alpha\}$  for the sparse representation of all patches.  $\sigma$  denotes the standard deviation of the Gaussian kernel which assigns a large weight to points that are closer to the center of the patch. It is defined by  $R$  and  $D\alpha$ .  $\|\alpha_{ij}\|_0^0$  denotes the  $l^0$  norm that counts the nonzero entries of vector  $\alpha$ , and  $L_0$  is the sparsity level that limits the maximum nonzero entry number in  $\alpha$ .

The numerical solution of the optimization problem (1) is obtained by a weighted version of the K-SVD algorithm [14]. It consists of two main steps:

$$\min_{D, \Gamma} \mu \sum_{ij} \|R_{ij}x - D\alpha_{ij}\|_{2, \sigma}^2 \quad \text{s.t. } \|\alpha_{ij}\|_0^0 \leq T \forall i, j$$

(2)

$$\min_x \|x - y\|_2^2 + \mu \sum_{ij} \|R_{ij}x - D\alpha_{ij}\|_{2, \sigma}^2$$

(3)

(2) aims to train the dictionary  $D$  and  $\Gamma$  from a set of image patches. It is solved with the K-means Singular Value Decomposition (K-SVD) after replacing  $x$  by the known observed image  $y$ . This operation is iteratively performed in two steps: (1) sparse coding of  $\Gamma$  (including all  $\{\alpha\}$ ) using the orthogonal matching pursuit (OMP) algorithm; (2) dictionary update by minimizing (2) with  $D$  being a matrix with unit-norm columns in order to avoid scaling ambiguity [15]. Given the dictionary  $D$ , we compute for each training image, the patch-wise representations  $\Gamma$  using the OMP algorithm. Finally, given  $D$  and  $\Gamma$ , we compute the output image  $x$  by solving (3) according to a simple least squares approach:

$$x = \left( I + \mu \sum_{ij} \sigma_{ij} \cdot R_{ij}^T R_{ij} \right)^{-1} \left( y + \mu \sum_{ij} \sigma_{ij} \cdot R_{ij}^T D \alpha_{ij} \right)$$

(4)

Contrary to what was pointed out in the literature, we found that the dictionary trained from a SDCT abdomen image always provided results that were visually close to LDCT images (when compared with the dictionary trained from the LDCT image itself). The reason is that most abdomen CT images have similar tissue compositions and the dictionary discrepancy often expresses a very few difference in the final sparsified features. In consequence, we decided to use a pre-computed general dictionary  $D$  (cf. Fig. 2.a for illustration) that was preliminary trained from a high quality SDCT abdomen reference image (Fig. 2.b). One interesting advantage of using this general dictionary is that the intensive computations, involved in the dictionary construction, are avoided. We also improved the original K-SVD algorithm by associating a weighting to each pixel in the extracted patches, which is function of its distance to the center of the patch (a large weight is given to points that are close to the centre of the window and decreases as the distance of the point increases).

We finally performed the optimization process using the dictionary  $D$  obtained from (2) and (3) and considering the following three steps:

$$\text{(S1), } \min_{\Gamma} \mu \sum_{ij} \|R_{ij}x - D_p \alpha_{ij}\|_{2, \sigma}^2 \quad \text{s.t. } \|R_{ij}x - D_p \alpha_{ij}\|_{2, \sigma}^2 \leq \epsilon \forall i, j$$

(5)

$$\text{(S2), } \min_x \|x - y\|_2^2 + \mu \sum_{ij} \|R_{ij}x - D_p \alpha_{ij}\|_{2, \sigma}^2$$

(6)

$$\text{(S3), } x^p = \text{unsharpFilter}(x, \kappa)$$

(7)

The sparse coefficients  $\Gamma$  and DL treated image  $x$  are calculated using (5) and (6). The  $\epsilon$  in (5) denotes the tolerance parameter used in the computation of the  $\Gamma$  coefficients. Step S3 (7) characterizes the final contrast enhancing unsharp filtering with the  $\kappa$ -weight kernel [16]:

-κ  
-κ  
-κ

-κ  
 $1+8κ$   
-κ

-κ  
-κ  
-κ

## EXPERIMENT

Approval of this study was granted by our institutional review board. A non-conflict of interest for this work was declared. SDCT images of abdomen were acquired on a multi-detector row Siemens Somatom Sensation 16 CT scanner with a current of 260mAs while LDCT images were obtained from a reduced current of 50 mAs. The scanning parameters were the following: kVp, 120; slice thickness, 5 mm; Gantry rotation time, 0.5s; detector configuration (detector rows  $\times$  section thickness), 16mm  $\times$  1.5mm ; table feed per gantry rotation, 24 mm; pitch, 1:1; reconstruction method: FBP algorithm with convolution kernel "B31f" ("B31f" is the routine smoothing kernel used in abdomen scans for Siemens CT). The windows and level setting were chosen to optimize the visualization of these data (center, 50HU; width, 350HU). For evaluation purpose, we compared the proposed method with the LNL method in [9]. The LNL method was accelerated using GPU (Graphics Processing Unit) techniques based on [9]. All the CT images were exported as DICOM files and then processed offline on a PC workstation (Intel Core™ 2 Quad CPU and 4096 Mb RAM, GPU (NVIDIA GTX465)) using Visual C++ as programming language (Visual Studio 2008 software; Microsoft).

For both algorithms, the parameter setting was completed applying a greedy algorithm to find the optimal parameter that provided the best qualitative results. This qualitative evaluation was carried out in collaboration with a radiologist (X. D.Y, 15 years clinical experience). These optimal parameters are listed in TABLE I with the computation time costs for each method.

To specify the computation cost at each different stages of the proposed DL-unsharp processing, we used K-step, O-step, I-step and F-step techniques to represent the K-SVD stage (2)–(3) (dictionary training), OMP step (5) (sparse coefficient estimation), the image update stage (6), and the unsharp filtering step (7), respectively. We see in Table I that the dictionary learning in the K-step method is computationally more time consuming than the O-step and I-step techniques. Si if we remove the K-step and replace it by a pre-trained global dictionary (Fig. 3(a)), the proposed implementation appears thus more efficient in computation time (2.28+ 0.96 +0.12 = 3.36 seconds) than the LNL method (8.07 seconds).

Fig. 3 and 4 illustrate the results for two patient datasets. Fig. 3 (a) and Fig. 4 (a) depict two abdomen LDCT images including tumors (pointed by red circles or arrows) of a 61 years old female and 56 years old male patient respectively. Fig. 3 and Fig. 4 (b), (c) and (d) show the corresponding SDCT, LNL processed LDCT and DL-unsharp processed LDCT images respectively. We observe that, under low dose scanning condition, mottled noise severely degrades the images and the tumor boundary appears fuzzy. Considering the SDCT images as references, we observe that the LNL processed images (Fig. 3 (c) and Fig. 4 (c)) have been smoothed but still contain noise and stripe artifacts. The result appears more convincing with the DL-unsharp method since we can observe a more efficient noise reduction with a good preservation of tumor structures (Fig. 3 (d) and Fig. 4 (d)). Their restoration provides a visual appearance of the texture that is close to those of the SDCT images. In the one including multiple hepatic metastases in Fig. 4, the DL-unsharp algorithm allows enhancing the small structures as the small lesions which appears better discriminated than in the LNL processed images (see arrows).

## CONCLUSION

The algorithm described here and named DL-unsharp is employed for improving abdomen LDCT image quality, the objective being both to suppress the mottled noise and streak artifacts while enhancing the structure edges especially on tumors or lesions. This method makes use of a patch based DL processing followed by a contrast restoration unsharp filtering. Furthermore, the dictionary training has been built from a set of abdomen SDCT images to optimize the algorithm performance. We demonstrated the potential of the proposed approach on abdomen tumor LDCT datasets. Experiment results showed the proposed approach can greatly improve the quality of images acquired with a reduced X-Ray dose by 80%.

However, some improvements are needed: First, the whole computation cost of the DL-unsharp processing still need to be accelerated to meet the clinical requirement (less than 0.5 second per image). Second some parameters are currently set empirically and need more experiments to validate their value. Thirdly, extensive experiments have to be led to confirm these preliminary results. In conclusion, future work will be devoted to all these points: parallelization of pair-wise operations, automatic estimation of the best parameters to optimize the tradeoff between data fidelity and priors and extensive evaluation.

## Acknowledgements:

This research was jointly supported by National Basic Research Program of China under grant (2010CB732503), National Natural Science Foundation under grant 81000636, and the Natural Science Foundations of Jiangsu Province (BK2011593) and the French National Institute for Health (INSERM).

## References:

- 1 . Kak AC , Slaney M . Principles of Computerized Tomographic Imaging . Philadelphia, PA SIAM ; 2001 ;
- 2 . Brenner DJ , Hall EJ . Computed tomography-an increasing source of radiation exposure . New England Journal of Medicine . 357 : 2277 - 2284 2007 ;
- 3 . Mannudeep K , Michael MM . Strategies for CT Radiation Dose Optimization . Radiology . 230 : 619 - 628 2004 ;
- 4 . Yazdi M , Beaulieu L . Artifacts in Spiral X-ray CT Scanners: Problems and Solutions . International Journal of Biological and Medical Sciences . 4 : 135 - 139 2008 ;

- 5 . Watanabe H , Kanematsu M , Miyoshi T . Improvement of image quality of low radiation dose abdominal CT by increasing contrast enhancement . AJR . 195 : 986 - 992 2010 ;
- 6 . Funama Y , Awai K , Miyazaki O , Nakayama Y , Goto T , Omi Y . Improvement of low-contrast detectability in low-dose hepatic multidetector computed tomography using a novel adaptive filter: evaluation with a computer-simulated liver including tumors . Invest Radiol . 41 : 1 - 7 2006 ;
- 7 . Wang J , Lu H , Wen J , Liang Z . Multiscale penalized weighted least-squares sinogram restoration for low-dose X-Ray computed tomography . IEEE T-BME . 55 : ( 3 ) 1022 - 1031 2008 ;
- 8 . Ehman E , Guimarães L , Fidler J , Takahashi N . Noise reduction to decrease radiation dose and improve conspicuity of hepatic lesions at contrast-enhanced 80-kV hepatic CT using projection space denoising . AJR . 198 : 405 - 411 2012 ;
- 9 . Chen Y , Luo L , Chen W . Improving Low-dose Abdominal CT Images by Weighted Intensity Averaging over Large-scale Neighborhoods . European Journal of Radiology . 80 : e42 - e49 2011 ;
- 10 . Lewic MS , Olshausen BA , Field DJ . Emergence of simple-cell receptive field properties by learning a sparse code for natural images . Nature . 381 : 1996 ; 607 - 609
- 11 . Lewicki MS . Learning overcomplete representations . Neural Comput . 12 : 2000 ; 337 - 365
- 12 . Delgado KK , Murray JF . Dictionary learning algorithms for sparse representation . Neural Comput . 15 : 349 - 396 2003 ;
- 13 . Donoho DL , Elad M . Maximal sparsity representation via  $l_1$  minimization . Proc Nat Aca Sci . 100 : 2197 - 2202 2003 ;
- 14 . Elad M , Aharon M . Image denoising via sparse and redundant representations over learned dictionaries . IEEE TIP . 15 : ( 12 ) 3736 - 3745 2006 ;
- 15 . Li S , Fang L , Yin H . An efficient dictionary learning algorithm and its application to 3-D medical image denoising . IEEE T-BME . 59 : ( 2 ) 417 - 427 2012 ;
- 16 . Haralick R , Shapiro L . Computer and Robot Vision . Addison-Wesley Publishing Company ; 1992 ;

**Fig 1**

Outline of the proposed DL-unsharp algorithm.

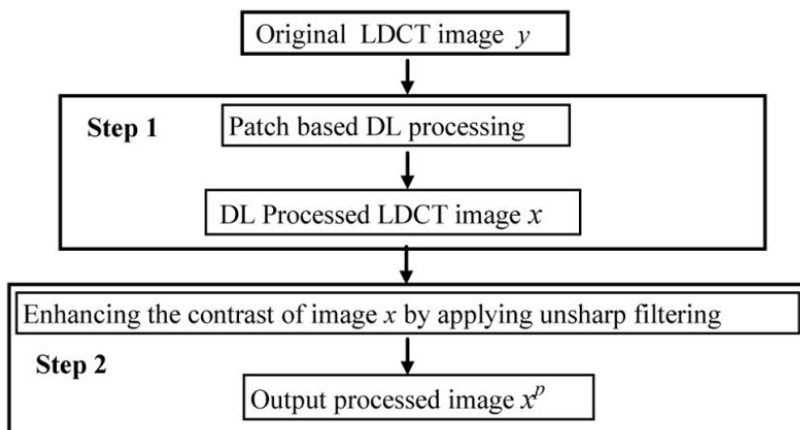
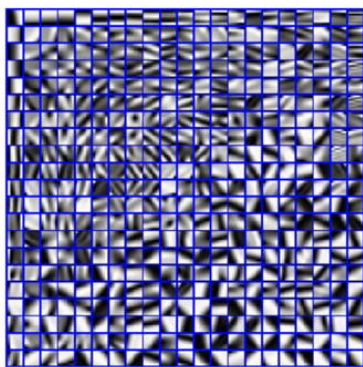
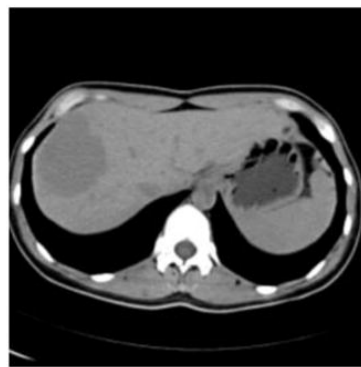


**Fig. 2**

(a) Dictionary example; (b) Abdomen SDCT image from which the dictionary has been trained.



a)



b)

**Fig. 3**

Results for a dataset of a 61 years female patient having a liver tumor (red circles). (a): original LDCT image; (b): SDCT image; (c): LNLN processed LDCT image; (d): DL-unsharp processed LDCT image.

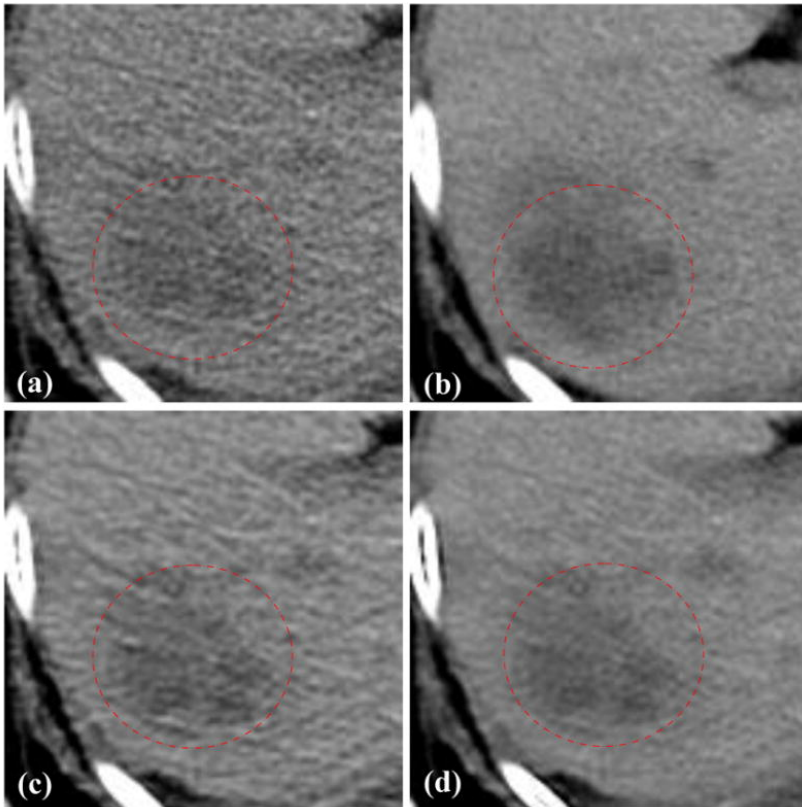


**Fig. 4**

Results for a dataset of one 56 years male patient having multiple hepatic metastases (red arrows) in the abdomen. (a): original LDCT image; (b): SDCT image; (c): LNLN processed LDCT image; (d): DL-unsharp processed LDCT image.

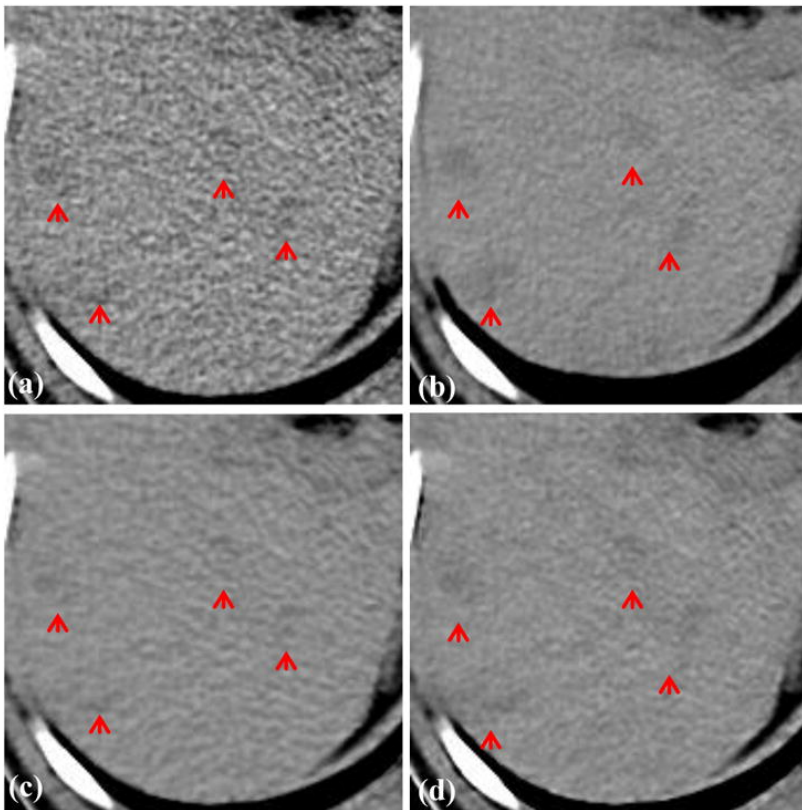


**TABLE I**

PARAMETER SETTING AND COMPUTATION COST (IN SECOND) FOR DIFFERENT METHODS

	<b>LNLM method</b>	<b>DL-unsharp method</b>			
Parameter setting	$h = 2$ , Patch size $N = 7 \times 7$ , Neighborhood size $N = 81 \times 81$	$K = 256$ , $N = 8 \times 8$ , $L_0 = 3$ , Iteration = 20, $T = 21$ , $\epsilon = 21$ , $\mu = 21$ Unsharp filter: $\kappa = 0.1$ ,			
Computation Cost (in second)	8.07	K-step 979,53	O-step 2,28	I-step 0.96	F-step 0.12